International Journal of Mechanical and Electrical Engineering
ISSN: 3005-9615 (Print), ISSN: 3005-7132 (Online) | Volume 7, Number 3, Year 2025
DOI: https://doi.org/10.62051/ijmee.v7n3.08
Journal homepage: https://wepub.org/index.php/IJMEE/index

Single Diamond Scratching of Cf/SiC Composite: Force and Material Removal Mechanism Study

Yonggang Zhang

School of Mechanical Engineering, Tianjin University of Technology and Education, Tianjin 300222, China

ABSTRACT

As one of the ceramic matrix composites (CMCs), carbon fiber-reinforced silicon carbide matrix (Cf/SiC) composites have become ideal materials for various engineering applications due to their outstanding properties. Precision surface grinding technology has been widely applied in the machining of CMC composites; however, the material removal mechanism of Cf/SiC composites remains incompletely elucidated. To reveal the material removal mechanism during the grinding of Cf/SiC composites, we designed and conducted single-abrasive scratch tests. Experimental parameters, particularly cutting speed, were aligned with actual grinding processes. Results indicate that grinding parameters—feed rate, cutting depth, and cutting direction—significantly influence grinding force and surface integrity. Impact at the tool tip and abrasive action are the primary causes of material removal. During the grinding of Cf/SiC composites, the predominant material removal mode is brittle fracture. This is because the damage behavior of Cf/SiC composites is primarily a combined manifestation of matrix cracking, fiber fracture, and fiber/matrix interface debonding. These findings are rationally explained based on the material properties and microstructural damage characteristics of the composites.

KEYWORDS

Cf/SiC Composite Materials; Scratch Direction; Damage.

1. INTRODUCTION

Carbon fiber-reinforced silicon carbide (Cf/SiC) composites have emerged as indispensable key materials for manufacturing hot-end components in aerospace engines and vehicle engines due to their outstanding

performance characteristics, playing a pivotal role in the development of related fields. Cf/SiC composites consist of fibers, an interface layer, and a SiC matrix [1]. Cf/SiC composites exhibit numerous superior properties: high and stable friction coefficients insensitive to variations in speed, load, and temperature; excellent wear resistance and break-in characteristics; strong environmental adaptability with corrosion, oil, and moisture resistance; favorable mechanical properties; low density; and extended service life[2], making them the preferred choice for next-generation high-performance friction materials.

Single-abrasive particle scratch tests can visually reveal various damage modes in Cf/SiC composites under single-particle action, such as matrix spalling, fiber cracking, fracture, and fiber pull-out. Based on analyzing the motion characteristics of single abrasive particles during grinding, Z. L. Zan et al.[3] investigated the scratching force and material removal mechanism when a single particle linearly scratched SiCf/SiC composites at different cutting depths. The study revealed that fiber orientation and weave structure significantly influence the material removal mechanism, scratching force, and

Content from this work may be used under the terms of CC BY-NC 4.0 licence (https://creativecommons.org/licenses/by-nc/4.0/).
Published by Warwick Evans Publishing.

surface damage. J F Yin and G Garcia Luna et al.[4,5] conducted single-abrasive circular trajectory scratching tests on ceramic matrix composites, varying factors such as abrasive shape, particle size, grinding speed, and fiber orientation to identify mechanisms influencing material removal during ceramic matrix composite grinding. J Chen et al.[6] conducted variable-load nano-scratch tests on one-dimensional Cf/SiC composites at different fiber orientations to analyze fiber fracture mechanisms and damage behavior transitions at the nanoscale. C Cao and Q Liu et al.[7] analyzed the effects of different fiber orientations on material removal patterns and scratching forces during single-abrasive-grain scratching from both simulation and experimental perspectives. Y Liu et al.[8] discussed the surface characteristics of abrasive wear and scratching grooves during the scratching process based on single-abrasive-grain scratching tests, revealing the material removal mechanism.

This study designed and conducted novel single-abrasive-grain scratching experiments. Surface damage induced by scratches in Cf/SiC composite specimens was investigated, exploring the relationship between scratch force and parameters such as feed rate, cutting depth, and cutting direction. By analyzing microstructural features at the fiber-matrix interface, the mechanism of material removal during Cf/SiC composite grinding was comprehensively elucidated. The study of microstructural effects in scratch tests further deepened the understanding of surface damage.

2. MATERIAL PREPARATION

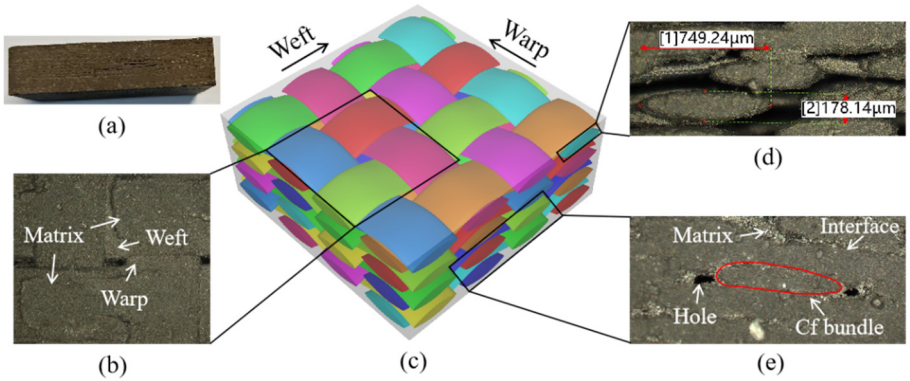

Figure 1. Structure of the Cf/SiC composite.

Table 1. Mechanical properties of the present Cf/SiC composite.

Parameter	Value
Temperature resistance/vacuum	1,600°C
Density	1.75 g/cm^3
Flexural strength	220 MPa
Compressive strength	9,149 MPa
Young's modulus	41,700 MPa
Tensile strength	293 MPa
Interlamination shear strength	12 MPa
Thermal conductivity	30W/mK
Coefficient of thermal expansion	0.09×10^{-6}K

The material used in this experiment was Cf/SiC composite, with sample dimensions of 40×25×10 (L×W×H) mm. Its macroscopic structural features are clearly observable in Figures 1 (a) and (c). The Cf/SiC composite primarily consists of carbon fibers, a silicon carbide matrix, and pyrolytic carbon

interfaces. As shown in Figures 1 (b) and (e), besides these three main components, certain pore defects exist at fiber junctions. This is attributed to insufficient penetration and filling of the silicon carbide matrix within the carbon fibers during preparation, resulting in a non-ideal density state. Figure 1 (d) displays the geometric morphology of a single carbon fiber bundle end face, exhibiting a typical elliptical shape. Detailed mechanical property data for the Cf/SiC composite material are listed in Table 1.

3. EXPERIMENTAL SETUP AND PROCEDURE

The single-grain scratch test employed a progressive deepening method with a scratch distance of 10 mm and a maximum scratch depth of 0.1 mm. The experimental apparatus is shown in Figure 2 . During testing, the Cf/SiC composite material was secured to a fixture, which was then placed on a triaxial piezoelectric force gauge. Scratch forces were recorded in real time using the DHDAS dynamic signal acquisition and analysis system on a computer. The force measurement system is depicted in Figure 2. The scratching force applied to the specimen comprises a normal force Fn (Fn = -Fz) and a tangential force Ft (Ft = -Fx or Ft = -Fy), with the selection of Ft depending on the actual tool feed direction. The diamond indenter used in the experiment was manufactured by Zhejiang Shengzuan Hardware Co., Ltd. The diamond grit featured a 120° tip angle, a cutting edge radius of 0.2 ± 0.01 mm, and a depth of 0.4 mm. Experimental data primarily encompass scratch force and scratch morphology. Scratch force was measured using a force gauge during testing. Finally, scanning electron microscopy (SEM) was employed to examine scratch morphology, revealing potential damage mechanisms in Cf/SiC composite materials during single-abrasive-grain scratching tests.

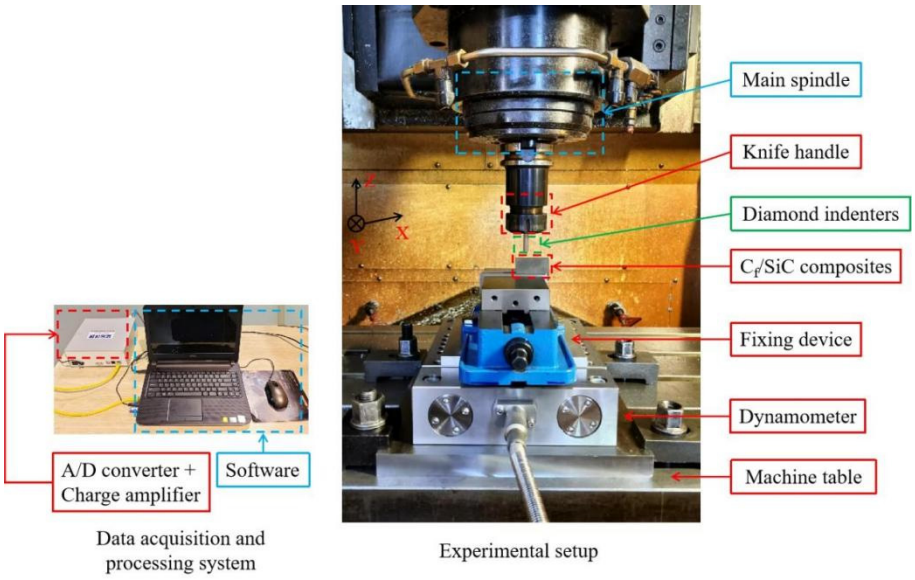

Figure 2. Single-grain scratching test: (a) Data acquisition and processing system and (b) Experimental setup.

Based on the relationship between scratch direction and fiber orientation, three typical scratch surfaces are defined: SA, SB, and SC surfaces, shown in Figures 3(a), (b), and (c), respectively. The SA surface features scratch directions along both transverse and longitudinal fibers; the SB surface has scratch directions along transverse fibers and perpendicular to fibers; the SC surface exhibits scratch directions along longitudinal fibers and perpendicular to fibers. At the start of the experiment, the spindle was slowly lowered along the negative Z-axis by adjusting the handwheel until the force gauge received a force signal, ensuring the diamond indenter contacted the Cf/SiC composite surface.

Scratch parameters are summarized in Table 2. For each combination of scratch parameters, three scratch tests were repeated with a 3 mm scratch spacing, and the average scratch force was recorded.

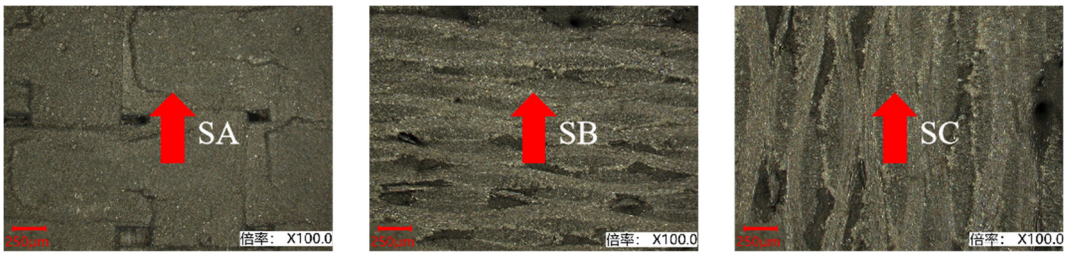

(a) (b) (c)

Figure 3. Definitions of scratched surfaces: (a) SA surface, (b) SB surface and (c) SC surface.

Table 2. Scratching parameters for single-grain scratching experiments.

Surfaces	Parameters	Values
SA, SB, SC	Scratching speed f [mm/min]	1500,3000,4500,6000
	Scratching depth ap [μm]	0-100

4. RESULTS AND DISCUSSION

4.1. Influence of Scratching Parameters on Cutting Force

The shear mode significantly influences scratch force, which is determined by the relative motion between particles and fibers. Typically, shear forces associated with three typical shear modes generally follow these rules: cutting along the fiber end face yields greater force than cutting along the fiber axis, while cutting perpendicular to the fiber direction produces the smallest force. Due to different combinations of shear modes, the scratch forces in three directions for 2D Cf/SiC composites exhibit significant differences.

Theoretically, when a diamond indenter scratches a surface, the volume of material removed per unit time increases with feed rate, leading to higher scratch force. Figure 4 illustrates the effect of feed rate on the average scratch force across the entire scratch distance. The normal force (Fn) and tangential force (Ft) exhibit distinct trends across SA, SB, and SC surfaces, though all show an overall upward trajectory. As the feed rate increased from 1500 mm/min to 3000 mm/min, the tangential force Ft on the SA surface first rose from 41.46 N to 44.72 N, then stabilized at 44.46 N at 4500 mm/min, before increasing again to 62.71 N at 6000 mm/min. Similarly, the normal force Fn increased from 41.50 N to 49.10 N, then decreased to 43.43 N, and finally increased to 58.73 N. Observations indicate that at a feed rate of 3000 mm/min, the scratch trajectory aligns directly above the warp and weft yarns. At 1500 mm/min and 4500 mm/min, however, scratches occur between adjacent warp fiber bundles. This corresponds to the indenter scraping perpendicular to the fiber direction, resulting in a scratch force trend that first increases and then decreases. Additionally, due to material preparation process limitations, voids exist in the orthogonally woven warp and weft yarns. If these voids result from insufficient SiC matrix filling, the scratch force exhibits a sudden drop followed by a sharp increase within an extremely short timeframe. This trend is particularly pronounced at feed rates of 1500 mm/min and 4500 mm/min. The normal force (Fn) and tangential force (Ft) on the SB surface exhibit a linear trend, both gradually increasing with feed rate from 21.72 N and 15.27 N to 49.73 N and 50.80 N, respectively. Notably, the normal force Fn and tangential force Ft on the SC surface exhibit divergent trends. At a feed rate of 3000 mm/min, Fn first increases

then decreases, while Ft first decreases then increases. However, the total scratching force remains relatively stable overall. Notably, the normal force Fn and tangential force Ft on the SC surface were significantly greater than those on the SA and SB surfaces, with scratch forces approximately twice as high. Observation reveals that the scratch depth formed on the SC surface during scratching is significantly deeper than that on the other two surfaces, with a maximum depth difference of approximately 1–2 times. Consequently, at the same depth, the SC surface removes a greater volume of material under the compressive and shear forces exerted by the diamond indenter, requiring a higher scratching force.

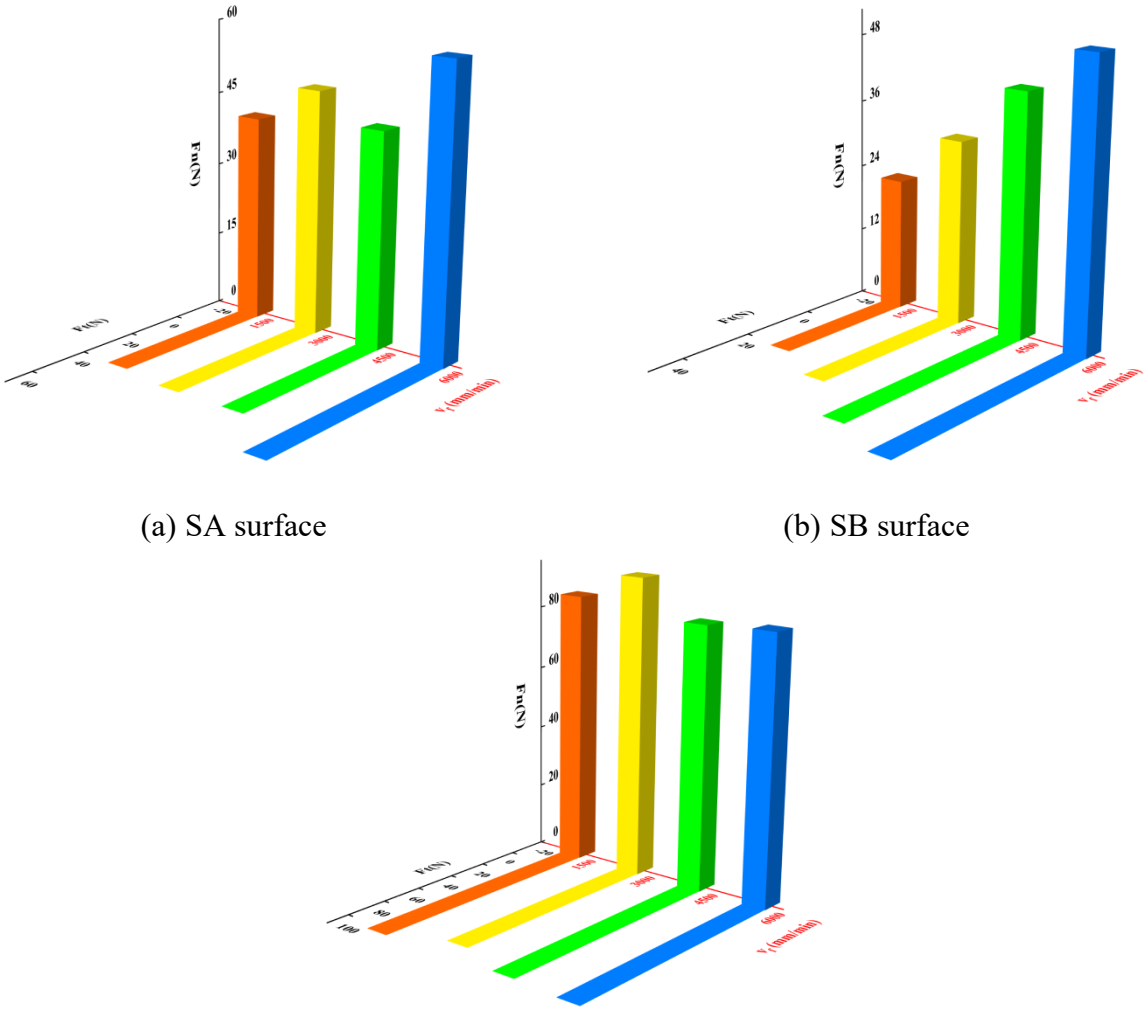

(a) SA surface

(b) SB surface

(c) SC surface

Figure 4. Effect of Scratch Speed on Scratch Force.

Figure 5 displays the scratch force waveforms for the SA, SB, and SC scratch surfaces over one cycle at a feed rate of 4500 mm/min. The waveform diagram visually reflects the influence of scratch depth on the trend of scratch force variation. It can be observed that the normal force Fn is slightly greater than the tangential force Ft in the SA and SB directions, while the tangential force Ft is slightly greater than the normal force Fn in the SC direction. Despite fluctuations, the overall trend for both normal force Fn and tangential force Ft across all three scratch surfaces is an increase with increasing scratch depth, attributable to the growing volume of material removed. The waveforms for SA and SB surfaces exhibit abrupt drops and rises, with the scratch force even reaching zero at approximately 60 μm scratch depth on the SB surface. This corresponds to the presence of pores mentioned earlier, resulting from material preparation. Furthermore, comparing the scratch force magnitudes across the

three directions reveals the following trend for maximum scratch force at identical scratch distances and depths: SC > SB > SA. This outcome primarily stems from constitutive material differences, where the radial elastic modulus and hardness of carbon fiber are lower than those in the axial direction.

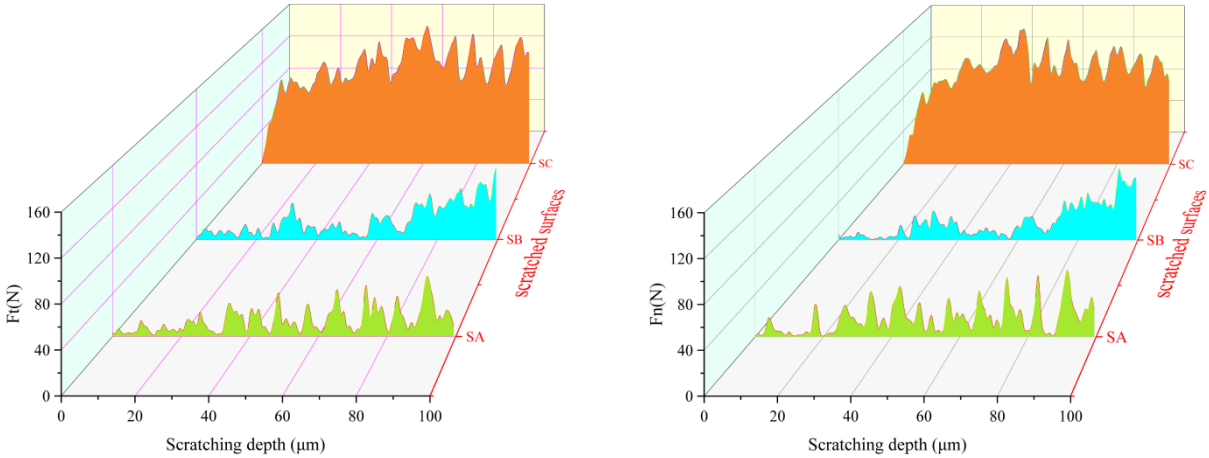

(a) Tangential force characteristic (b) Normal force characteristic

Figure 5. The Scratching force waveform at 4500mm/min.

4.2. Characteristics of Scratched Surfaces and Removal Mechanisms

Figures 6-8 present SEM images of scratch surfaces on SA, SB, and SC substrates at a feed rate of 3000 mm/min. Each scratch surface clearly exhibits brittle removal, yet differences persist in the removal patterns of fiber orientation and composition within the scratched regions, as described below.

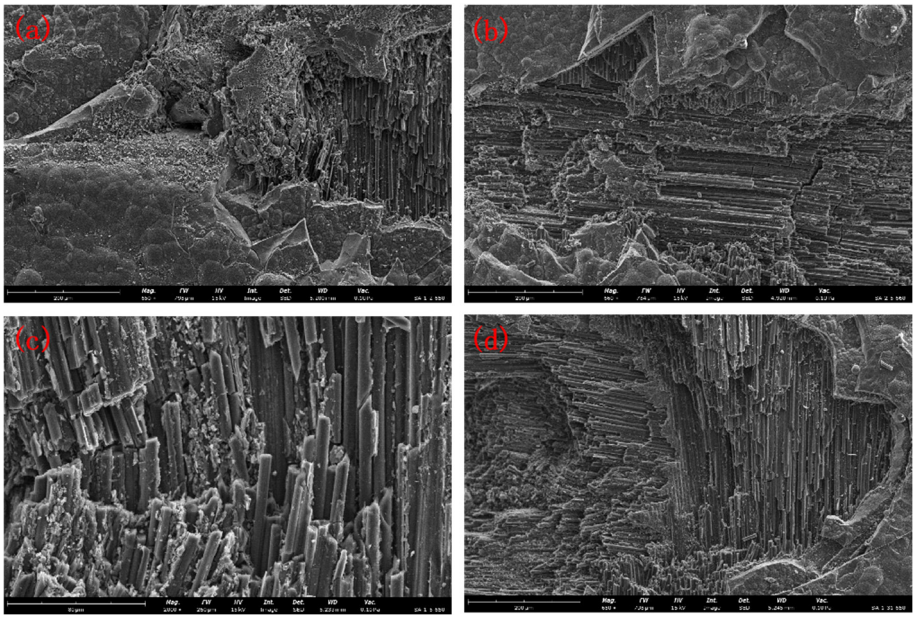

Figure 6. SEM images of scratches on the SA surface: (a) cutting edge; (b) transverse fibers; (c) longitudinal fibers; (d) cut-off edge.

Figure 6 illustrates the microstructure of scratches on the SA surface. As shown in Figure 6(a), the diamond indenter contacts the silicon carbide substrate before penetrating the fibers, resulting in pronounced brittle fracture and cracking of the substrate. Damage at the substrate-fiber interface manifests as substrate fragmentation. Figure 6(b) depicts the diamond indenter penetrating

longitudinal fibers, representing a typical penetration zone. Due to axial bending deformation, most silicon carbide fibers were removed via brittle fracture, exhibiting rough fracture surfaces. Some silicon carbide fibers displayed distinct plow furrow regions on their surfaces due to plastic deformation occurring at shallow depths. As cracks propagated along the entire fiber, the silicon carbide fibers were progressively removed. A small fraction of silicon carbide fibers underwent plow furrow-free brittle fracture, presenting relatively flat fracture surfaces. Additionally, fiber/matrix debonding accompanies the removal of silicon carbide fibers. As shown in Figure 6(c), carbon fibers undergo lateral bending deformation under diamond indenter compression and debond from the silicon carbide matrix, exhibiting clear signs of brittle fracture. Fibers are pulled out, leaving residual fibers, with direct fracture occurring at the bottom of the scratch. As shown in Figure 6(d), in the cutting region where the diamond indenter severed longitudinal fibers, carbon fibers were removed along their axial direction via brittle fracture, yielding relatively flat fracture surfaces. Some carbon fibers exhibited distinct signs of direct fracture, likely due to through-cracking. Additionally, some fractured fibers underwent fiber pull-out, leaving exposed fiber grooves.

The SEM image of surface scratches on the SB surface of the Cf/SiC composite is shown in Figure 7. As seen in Figure 7(a), when scratching perpendicular to the fibers at a shallow scratch depth, the fibers slide and pile up on both sides. Due to crack initiation, micro-brittle fracture occurs on the carbon fiber surface. As shown in Figure 7(b), the carbon fibers are removed through brittle fracture induced by bending failure, resulting in relatively smooth fracture surfaces. Additionally, it can be observed that bending-induced fracture of carbon fibers leads to fiber/matrix debonding. Scratch defects, such as fiber pull-outs and fiber exposure, are present on the scratched surface. As shown in Figure 7(c), the scratched region exhibits significant matrix damage and fiber pull-outs. Under the combined action of scratching force and pressure, some fiber bundles fail collectively along the fiber direction; longitudinal cracks initiate, causing the fiber bundles to split along the end face direction. As shown in Figure 7(d), in the cutting region where the diamond indenter severed longitudinal fibers, exposed fibers appeared in the left area due to the retraction process, accompanied by the formation of transverse cracks. Additionally, the right fibers exhibited significant interfacial delamination and extensive fiber fracture.

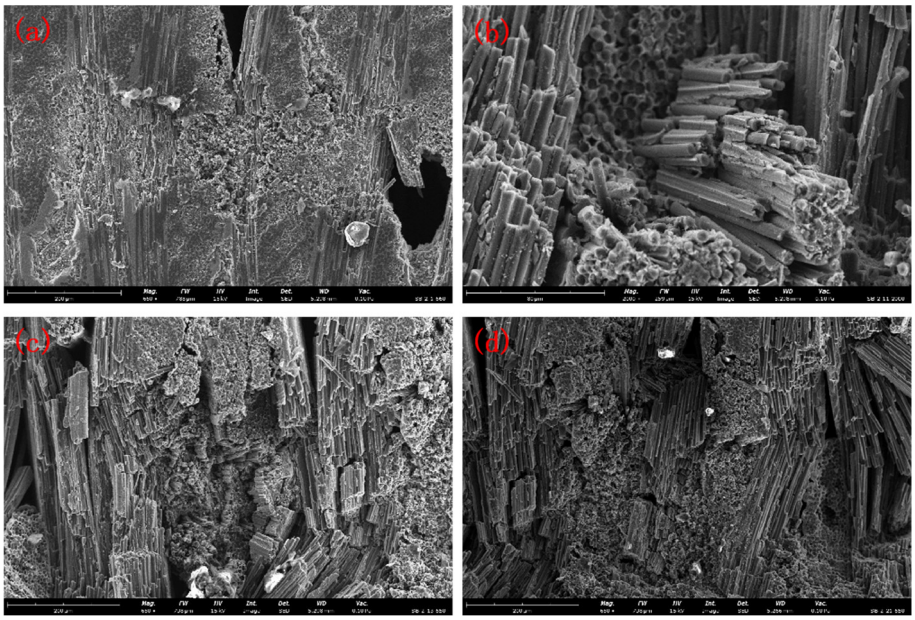

Figure 7. SEM images of scratches on the SA surface: (a) cutting edge; (b) transverse fibers; (c) longitudinal fibers; (d) cut-off edge.

Figure 8 presents SEM images of surface scratches on the SC surface of the Cf/SiC composite. As shown in Figure 8(a) and (b), carbon fiber removal occurs via brittle fracture, with composite defects

manifesting as fiber pull-outs, fiber exposure, matrix fragmentation, debris retention, and interfacial debonding. As evident in Figures 8(c) and (d), direct fracture of carbon fibers on the SC surface intensifies. Other scratch results exhibiting removal patterns and damage features resemble those described in Figures 6(a) and (b): carbon fibers are removed via brittle fracture, with rougher fracture surfaces in the incision zone and smoother fracture surfaces in the notch region.

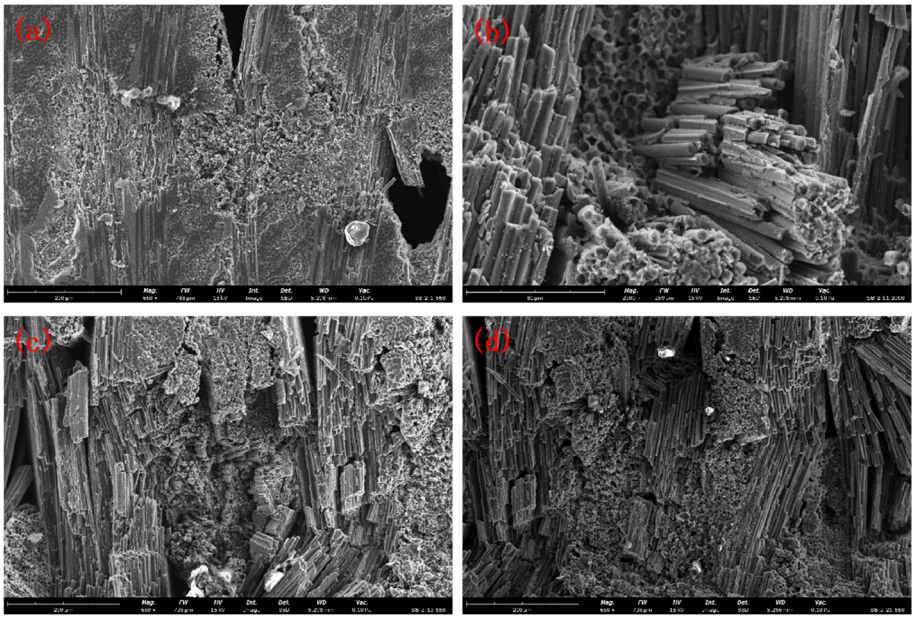

Figure 8. SEM images of scratches on the SA surface: (a) cutting edge; (b) transverse fibers; (c) longitudinal fibers; (d) cut-off edge.

5. SUMMARY

This study clearly demonstrates the material removal characteristics of Cf/SiC composites in single-particle scratch tests. Similar to actual grinding processes, the effects of single-particle grinding parameters were investigated. Based on these findings, grinding forces and surface integrity of Cf/SiC composites can be predicted. The results provide critical insights for grinding optimization. During scratching, cutting forces progressively increase with cutting depth. Findings indicate brittle fracture as the primary material removal mechanism in Cf/SiC composite grinding. Multiple damage behaviors-including significant matrix brittle damage, fiber fracture, fiber pull-out, and interfacial debonding-contribute to explaining the material removal mechanism. Cross-sectional surfaces exhibit a V-shaped profile in the transverse scratch direction and an arc-shaped profile in the longitudinal scratch direction. This phenomenon indicates that cutting forces and cutting directions influence material failure modes and surface-affected zones.

CONFLICTS OF INTEREST

The authors declare that they have no conflict of interest.

REFERENCES

[1] Zhang Z,Yuan S,Li Q,et al. Investigation on the machined surface quality and removal mechanism of SiCf/SiC composites in ultrasonic-assisted grinding. Int J Adv Manuf Technol 123, 4427-4445 (2022).

[2] Dayanand, S., Boppana, S.B. (2024). A Review on Conventional Machining Challenges of Ceramic Matrix Composites. In: Boppana, S.B., Ramachandra, C.G., Kumar, K.P., Ramesh, S. (eds) Structural Composite Materials. Composites Science and Technology . Springer, Singapore.

[3] Z.L. Zan, K. Guo, J. Sun, Y. Lu, B. Yang, X.J. Jia, V. Sivalingam, J.R. Xi, Investigation on scratching force and material removal mechanism of 3D SiCf/ C–SiC composites during single grain scratching, J. Eur. Ceram. Soc. 42 (2022) 5366–5379.

[4] J.F. Yin, J.H. Xu, W.F. Ding, H.H. Su, Effects of grinding speed on the material removal mechanism in single grain grinding of SiCf/SiC ceramic matrix composite, Ceram. Int. 47 (2021) 12795–12802.

[5] G. Garcia Luna, D. Axinte, D. Novovic, Influence of grit geometry and fibre orientation on the abrasive material removal mechanisms of SiC/SiC Ceramic Matrix Composites (CMCs), Int. J. Mach. Tools Manuf. 157 (2020) 103580.

[6] J. Chen, Q.L. An, M. Chen, Transformation of fracture mechanism and damage behavior of ceramic-matrix composites during nano-scratching, Compos. Part A Appl. Sci. Manuf. 130 (2020) 105756.

[7] C. Cao, Q.H. Song, H. Fu, H.S. Ji, Z.Q. Liu, L.P. Jiang, Fiber orientation effects on grinding characteristics and removal mechanism of 2.5D Cf/SiC composites, Chin. J. Aeronaut. 36 (2023) 425–441.

[8] Y. Liu, Y. Quan, C.J. Wu, L.Z. Ye, X.J. Zhu, Single diamond scribing of SiCf/SiC composite: Force and material removal mechanism study, Ceram. Int. 47 (2021) 27702–27709.